

ANALYSIS OF PHASE TRANSFORMATION IN HIPOEUTECTIC Al-Si ALLOYS

I. LICHIOIU¹ B. VARGA¹ V. GEAMĂN¹

Abstract: *Measurement of temperature and transformation duration provides information on structure generation. Improving the structure of hypoeutectic Al-Si alloys can be achieved both by introducing small quantities of additives and by applying high cooling rates. Dilatometric studies allowed determination of activation energy for the decomposition of supersaturated α solid solution. Increased cooling rates cause an increase of the activation energy from a value of 152 kJ/mol for casting in refractory brick to a value of 201 kJ/mol for casting in steel mould in case of ATSi5Cu1 alloy.*

Key words: *silumin, cooling rate, dilatometry, activation energy.*

1. Introduction

Al-Si alloys, the most important aluminium based metal materials used in foundries are known for their very good castability and adequate mechanical properties; further, these alloys have a very good corrosion strength, are easily machined by cutting processes and have a good weldability.

Form and dimensions of eutectic silicon crystals generated during solidification have an unfavourable effect on silumin properties, due to the growth effect as well as to the high fragility and hardness of this non-metallic phase.

In order to improve the structure and consequently to improve the mechanical and technological properties of hypoeutectic silumins, prior to casting these alloys are subjected to certain treatments aimed at improving their structure. Such treatments involve introducing of small quantities of additives for both globulization

of the eutectic silicon and crystalline refinement. The eutectic silicon form is modified by means of superficially active elements such as: Na, Sr, while the refinement of the solid solution dendrites is achieved by hard fusible elements such as Ti, B etc.

Modification of the form of silicon can also be achieved by applying high cooling rates. It has to be pointed out, that at high cooling rates, the proportion of Si in α solid solution increases over the 1.65%, value which is indicated in the thermal equilibrium diagram. In this case α solid solution becomes oversaturated, the generated structure being metastable [2].

2. Experimental Determination

The analyses of the untreated ATSi5Cu1 and ATSi8Cu3 hypo-eutectic alloys reported in this paper were conducted by simple thermal analysis, microscopic study and dilatometric analysis. The latter has allowed

¹ Dept. of Technological Equipment and Materials Science, *Transilvania* University of Braşov.

determining of the activation energy related to the decomposition of the supersaturated α solid solution into Si.

The ATSi5Cu1 and ATSi8Cu3 alloys were melted in an electric furnace with graphite crucible; subsequently ATSi8Cu3 was cast in graphite and refractory brick moulds and ATSi5Cu1 in steel and refractory brick moulds, respectively. Dimensions of the cast test pieces were: the first ones cast in refractory brick

moulds - $\varnothing 50 \times 60$ mm, the second ones cast in graphite moulds - $\varnothing 30 \times 70$ mm, and the third ones cast in steel moulds - $14 \times 80 \times 160$ mm respectively. Melted charges of untreated alloys were followed by alloys treated with master alloys, namely Al-Sr10 in the case of ATSi8Cu3 and Al-Ti5-B1 in the case of ATSi5Cu, by means of added them in the melt. Table 1 displays the chemical composition of the main elements, the weights of charges and additive materials.

Chemical composition, the weights of charges and additive materials Table 1

No.	ATSi8Cu3 [g]	ATSi5Cu1 [g]	AlSr10 [g]	AlTi5B1 [g]	Chemical composition [%]					
					Al	Si	Cu	Fe	Sr	Ti
1	1440	-	-	-	87.39	7.99	2.29	0.57	-	-
2	900	-	4.85	-	87.24	8	2.32	0.59	0.05	-
3	-	886	-	-	90.93	5.59	1.65	0.66	-	-
4	-	890	-	35.60	92	4.75	1.37	0.59	-	0.2

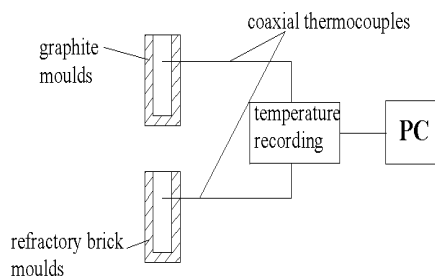


Fig. 1. Principle diagram of a thermal analysis

The experimental arrangement from Figure 1 was used for plotting the cooling curves.

Temperature was recorded by means of an EBI-2T-1202-TYPK logger, using coaxial thermocouples type K-TPN-101 with a diameter of 0.6 mm. The experimental data were processed by the EBI-WINLOG 2000-S software and OriginPro. Dilatometric studies were conducted by means of a LINSEIS L75/230 dilatometer.

3. Experimental Results

The cooling curves obtained for ATSi5Cu1 and ATSi8Cu3 untreated respectively treated

alloys for three cooling conditions are present in Figures 2 and 3.

The cooling conditions for each casting mould type were considered by the cooling rates in liquid state, computed with:

$$v_r^l = \frac{\Delta T}{\Delta \tau}, \quad (1)$$

where: ΔT - the temperature variations; $\Delta \tau$ - the time variations.

The temperatures highlighted on the cooling curves of Figures 2 and 3 correspond to the separation of α solid solution crystals, the eutectic and other intermetallic compounds (e.g. CuAl2 for ATSi8Cu3). The occurrence of undercooling phenomenon interfering before the primary crystallization can be observed on the curves corresponding to slow cooling rates.

Undercooling disappears in the case of ATSi5Cu1 treated with hard fusible elements (Ti + B) for structure finishing (Figure 2b - curve 1), what is in agreement with the general theory on the structure finishing mechanism with hard fusible elements by means of heterogeneous germination.

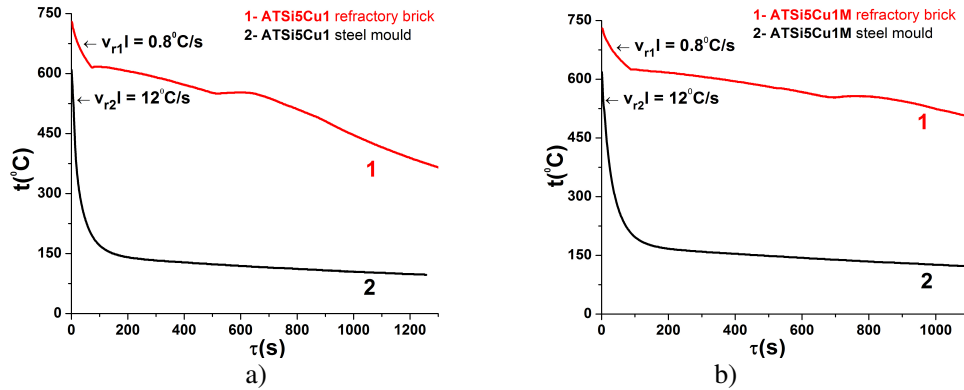


Fig. 2. Cooling curves for AlSi5Cu1 alloy cast in steel and refractory brick moulds: untreated alloy (a), treated alloy with Al-Ti5-B1 master alloy (b)

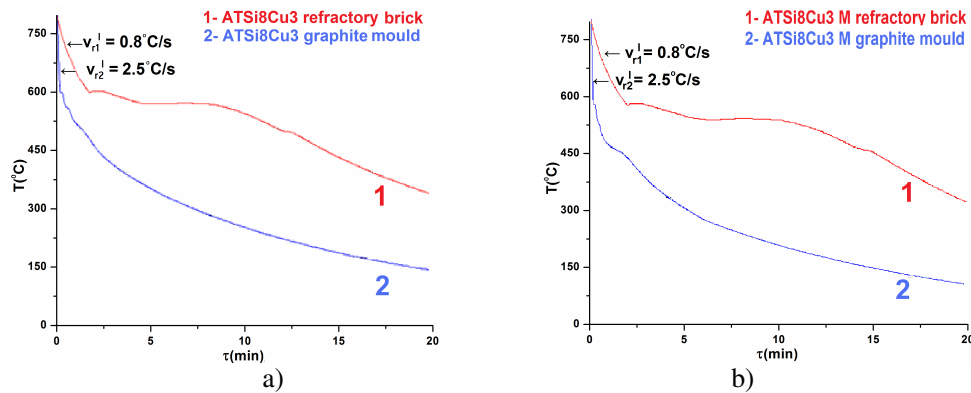


Fig. 3. Cooling curves for AlSi8Cu3 alloy cast in graphite and refractory brick moulds: untreated alloy (a), treated (modified) alloy with Al-Sr10 master alloy (b)

The addition of Sr causes changes of the cooling curve (Figure 3b) by extending the time required for the eutectic reaction. At the structure level Sr has a strong impact on the shape of the silicon crystals [3].

Figures 4 and 5 present the microstructures of the AlSi8Cu3 alloy modified with 0.05% Sr, after the adequate metallographic preparation of the samples.

In the case of the casting into moulds which ensuring slow cooling rates, the effect of Sr modification on parts properties is diminished by the presence of coarse intermetallic compounds. The presented alloy structures reveal that only the cumulated

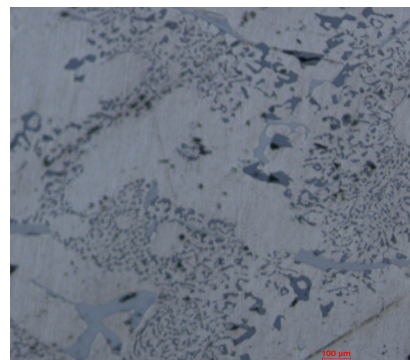


Fig. 4. Microstructure of AlSi8Cu3 alloy modified with 0.05% Sr cast in refractory brick mould

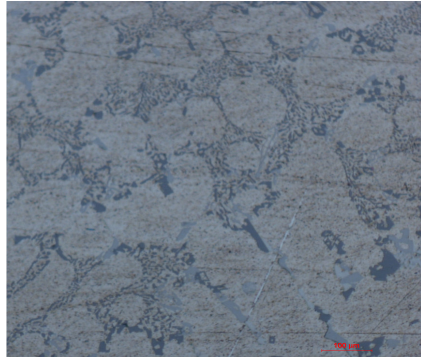


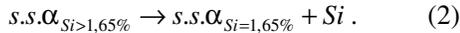
Fig. 5. Microstructure of AlSi8Cu3 alloy modified with 0.05% Sr cast in graphite mould

effects of Sr modification and graphite mould casting (high cooling rate) ensure an adequate modification of the eutectic Si and a fine distribution of the intermetallic compounds.

The results of the dilatometric analysis are presented in Figures 6 and 7 for ATSi8Cu3, and Figures 8-11 for ATSi5Cu1, respectively.

The dilatation curves reveal that the heating process of the alloy with cast structures causes the separation of Si from the supersaturated α solid solution and its deposition on the Si separations existing in the eutectic.

The separation of the Si from the supersaturated s.s. α can be represented as follows:



This transformation occurs accompanied by an increase in volume, clearly highlighted by the first derivative of the dilatation curve.

The curves of Figure 6 reveal that in the presence of strontium, the decomposition of the supersaturated solid solution takes place as in the unmodified alloy. Structural transformations cease to occur at cooling rates of 5 °C/min of the modified alloy (Figure 7).

The activation energy (E_a) is determined by the Kissinger equation [1], written as:

$$\frac{d\left(\ln \frac{v}{T}\right)}{d\left(\frac{1}{T}\right)} = -\frac{E_a}{R}, \quad (3)$$

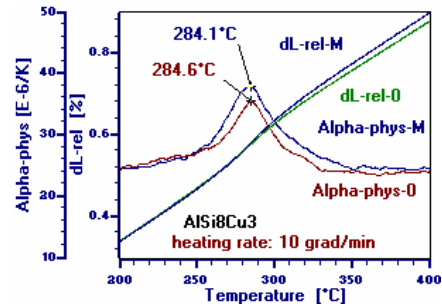


Fig. 6. Dilatation curves and dilatation coefficient for ATSi8Cu3 unmodified (0) and modified alloy (M)

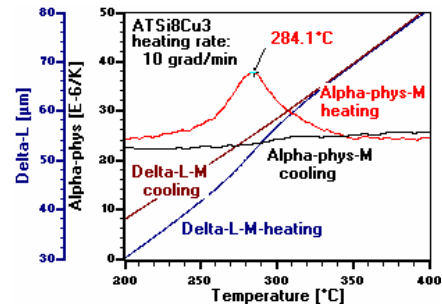


Fig. 7. Dilatation and contraction curves, and dilatation and contraction coefficients, respectively for ATSi8Cu3 modified alloy

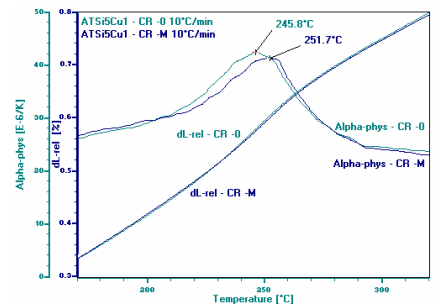


Fig. 8. Dilatation curves and dilatation coefficient for ATSi5Cu1 untreated (0) and the treated alloy (M) cast in refractory brick mould

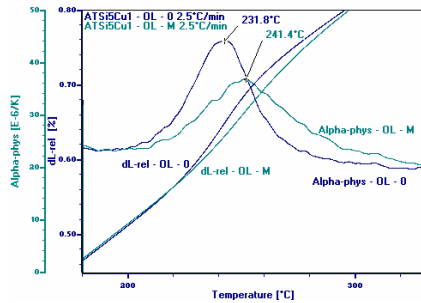


Fig. 9. Dilatation curves and dilatation coefficient for ATSi5Cu1 untreated (0) and the treated alloy (M) cast in steel mould

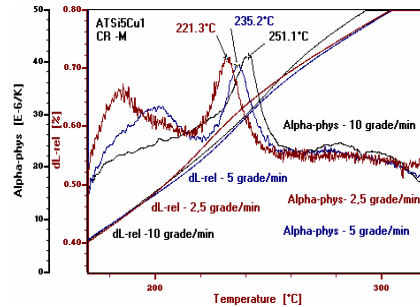


Fig. 11. Dilatation curves and dilatation coefficient for ATSi5Cu1 treated alloy cast in refractory brick mould, heated at different rates

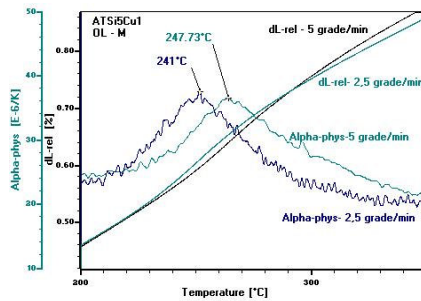


Fig. 10. Dilatation curves and dilatation coefficient for ATSi5Cu1 treated alloy cast in steel mould, heated at different rates

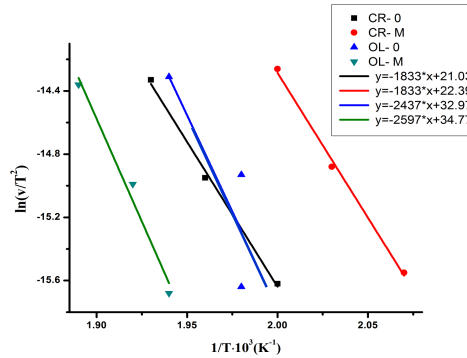


Fig. 12. Determination of the activation energy by graphic representation for ATSi5Cu1 alloy

where: T - the temperature corresponding to the peaks on the derivatives of the dilatation curves [°C]; v - cooling rate [°C/s]; E_a - activation energy [J/mol]; R - gas constant: 8.3144 [J/K·mol].

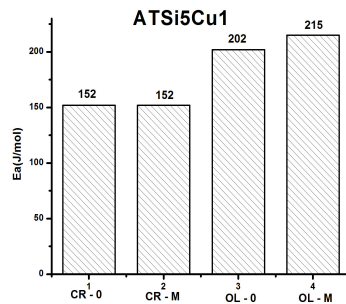


Fig. 13. Activation energies for ATSi5Cu1 alloy processed under different conditions

The temperatures corresponding to the peaks on the derivatives of the ATSi5Cu1 dilatation curves were used for determining the activation energy. Tables 2 and 3 feature the experimental and computed values required for plotting the $\ln\left(\frac{v}{T^2}\right) = f\left(\frac{1}{T}\right)$ diagrams.

4. Conclusions

Treating liquid alloys with hard fusible elements eliminates the undercooling phenomenon.

Dilatometric analysis reveals the importance of heat treatments for dimensions stabilizing applied to unmodified and modified silumins in order to avoid dimensional modifications caused by the

Experimental results and computed quantities for ATSi5Cu1-M Table 2

Parameters	Casting condition					
	Steel mould			Refractory brick mould		
v [°C/min]	2.5	5	10	2.5	5	10
v [°C/s]	0.041	0.083	0.16	0.041	0.083	0.16
t [°C]	241.4	247.7	254.4	211	219.5	228
T [K]	514.4	520.7	527.4	484	492.5	501
$\frac{1}{T} \cdot 10^3$ [K ⁻¹]	1.94	1.92	1.89	2.07	2.03	2
$T^2 \cdot 10^{-5}$ [K ²]	2.64	2.71	2.78	2.34	2.42	2.51
$\frac{v}{T^2} \cdot 10^7$ [s ⁻¹ K]	1.54	3.06	5.75	1.75	3.43	6.37
$\ln\left(\frac{v}{T^2}\right)$	-15.68	-14.99	-14.36	-15.55	-14.88	-14.26
E_a [kJ/mol]	215			152		

Experimental results and computed quantities for ATSi5Cu1-0 Table 3

Parameters	Casting condition					
	Steel mould			Refractory brick mould		
v [°C/min]	2.5	5	10	2.5	5	10
v [°C/s]	0.041	0.083	0.16	0.041	0.083	0.16
t [°C]	231.8	231	241.5	226	235.7	245.1
T [K]	504.8	504	514.5	499	508.7	518.1
$\frac{1}{T} \cdot 10^3$ [K ⁻¹]	1.98	1.98	1.94	2	1.96	1.93
$T^2 \cdot 10^{-5}$ [K ²]	2.54	2.54	2.64	2.49	2.58	2.68
$\frac{v}{T^2} \cdot 10^7$ [s ⁻¹ K]	1.6	3.26	6.04	1.64	3.2	5.96
$\ln\left(\frac{v}{T^2}\right)$	-15.64	-14.93	-14.31	-15.62	-14.95	-14.33
E_a [kJ/mol]	202			152		

transformation of the metastable structure of the deployed material. The phenomenon is of major importance for parts of high dimensional accuracy.

Increased cooling rates cause an increase of the activation energy for decomposition of supersaturated α solid solution in Si.

Acknowledgements

This paper is supported by the Sectoral Operational Programme Human Resources Development (SOP HRD), ID59321 financed from the European Social Fund and by the Romanian Government.

References

1. Kissinger, H.E.: *Reaction Kinetics in Differential Thermal Analysis*. In: *Analytical Chemistry* **29** (1957) No. 11, p. 1702-1706.
2. Lasagni, F., Falahati, A., et al.: *Precipitation of Si Revealed by Dilatometry in Al-Si-Cu/Mg Alloys*. In: *Kovove Materialy* **46** (2008) No. 1, p. 1-6.
3. Tenekedjiev, N., Closset, B., et al.: *Microstructures and Thermal Analysis of Strontium-Treated Aluminum-Silicon Alloys*. Ed. by Thomas S., American Foundrymen's Society, USA, 1995.